Available online at www.sciencedirect.com
ScienceDirect
Cement and Concrete Research 38 (2008) 290–299
Cement and Concrete Research

Mass and momentum interface equilibrium by molecular modeling. Simulating AFM adhesion between (120) gypsum faces in a saturated solution and consequences on gypsum cohesion

Paul Jouanna [a,b,*], Laurent Pèdesseau [a,c], Gérard Pèpe [b], David Mainprice [a]

[a] Géosciences Montpellier, Université Montpellier 2, CNRS, CC.60, 34095 Montpellier, France
[b] UMR CNRS 6114, Laboratoire GCOM2, Faculté des Sciences de Luminy, France
[c] INSA Rennes, MNT, 20 Avenue des Buttes de Coësmes, 35043 Rennes, France

Received 26 June 2006; accepted 19 September 2007

Abstract

Properties of composite materials depend on interatomic phenomena occurring between binder crystals. Experimental information of Atomic Force Microscopy (A.F.M.) is of prime importance; however understanding is helped by molecular modeling. As underlined in Section 1, the present study is able to simulate crystal interfaces in presence of a solution within apertures less than 1 Nanometer at a full atomic scale. Section 2 presents the case study of a gypsum solution between (120) gypsum faces, with related boundary conditions and atomic interactions. Section 3 deals with the mass equilibrium of the solution within interfaces <5 Å, using the original Semi Analytical Stochastic Perturbations (SASP) approach. This information becomes in Section 4 the key for explaining the peak of adhesion obtained in A.F.M. around an aperture of 3 Å and gives enlightenments on gypsum cohesion. In conclusion, this illustration shows the potentialities of full atomic modeling which could not be attained by any numerical approach at a mesoscopic scale.

Keywords: Microstructure; Bond strength; Micromechanics; Sulfate; Modeling

1. Introduction

1.1. Presentation

Mechanical properties of materials, of prime importance in many industrial research and development fields, are traditionally studied by a phenomenological approach at the macroscopic scale. For example, in the field of binders (plaster, cement) used in composite geomaterials of civil engineering, the fundamental property of cohesion is traditionally studied via the global resistance of the material considered as a black box. Such a phenomenological approach is not able to give the physical origin of this property and is thus an obstacle in the manufacturing of the composite materials. Similarly in geology, the properties of rocks are related to the cohesion between minerals and this property is fundamental for understanding the formation and evolution of rocks. A basic understanding of such a mechanical property is obviously linked to phenomena occurring at a nanoscale.

Experimental research has been very active at smaller and smaller scales for half a century. The first surface adhesion forces were observed in experiments thanks to the SFA "Surfaces Apparatus Force" [1] and [2]. It made it possible to establish the limits of the Derjaguin-Landau-Verwey-Overbeek (DLVO) theory [3] and to measure the Non-DLVO forces of hydration and the ionic correlation forces. However, the SFA method restricts the study to the adhesion forces on plane and thin surfaces. Such an historical tendency is observed in investigations of gypsum, a material of prime importance in civil engineering and considered in the case study presented below. The first study of interaction between gypsum crystals was performed via a "magneto-electric microdynanometer" [4]. In the last decade, direct interaction forces have been measured between a face and

* Corresponding author. Géosciences Montpellier, Université Montpellier 2, CNRS, CC.60, 34095 Montpellier, France.
E-mail address: jouanna@msem.univ-montp2.fr (P. Jouanna).

0008-8846/$ - see front matter © 2007 Elsevier Ltd. All rights reserved.
doi:10.1016/j.cemconres.2007.09.022

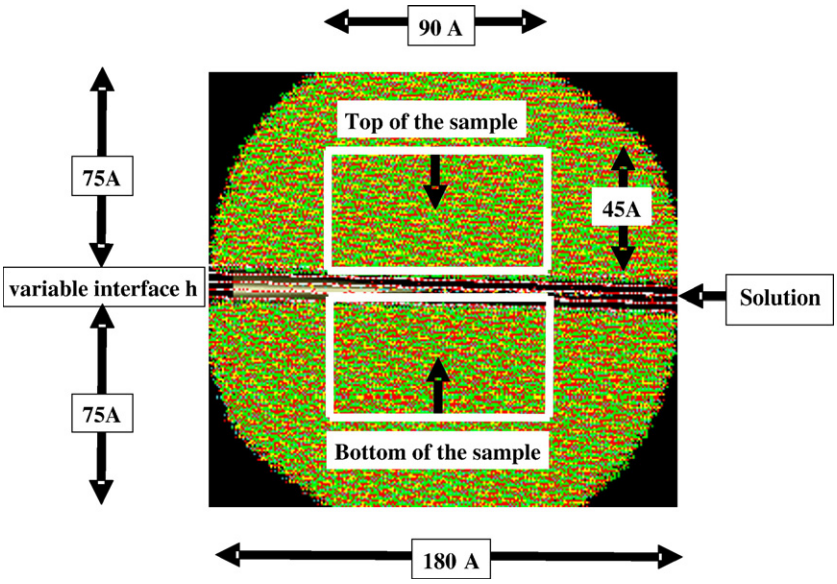

Fig. 1. Interface between two gypsum hemispheres. (For interpretation of the references to colour in this figure legend, the reader is referred to the web version of this article.)

a sphere in solution by A.F.M. (Atomic Force Microscopy) technology [5]. More recently, adhesion between two gypsum faces was investigated at the nanoscale [6] leading to comprehensive data on adhesion between (010), (120) and (−101) gypsum faces, with different relative orientations, in various solutions or in wet air [7]. Even if an effort is made to decrease the face size, A.F.M. experiments are still limited to relatively large surfaces (20 μm × 20 μm down to 2 μm × 2 μm). The roughness of the crystal faces impedes to know the exact "efficient contact area" between the probe and the sample, the measured stress being much lower than the "effective adhesion stress".

To help understanding experimental results, parallel improvements in modeling were limited by the lack of methods able to give the fluid description within the crystal interface at small apertures, where the maximum attraction is experimentally observed. Semi-continuous methods such as the DLVO theory are not useful at less than 10 Å and new modeling tools are to be developed at a complete atomic scale for the crystal, the solvent and the solute ions. Such studies are just emerging, in particular in the field of civil engineering materials, such as cement materials or gypsum [8].

1.2. Proposition

For demonstrating the possibility of obtaining information on cohesion at a complete atomic scale, this paper presents a chemical and mechanical modeling of a schematic A.F.M. test between two parallel crystal faces. For convenience, gypsum has been chosen as a reference crystal material for reasons of its molecular simplicity and the completeness of available experimental data, the solution being in equilibrium with the crystal. Section 2 presents the numerical *construction of the crystal interface*. Section 3 leads to the implementation of a solution within the crystal interface; the *mass equilibrium* of the interface solution is obtained by applying the Semi Analytical Stochastic Perturbations (S.A.S.P.) algorithm [9]. Finally Section 4 addresses the *momentum equilibrium* of the crystal faces and leads to the forces necessary to ensure the mechanical equilibrium of a chemically equilibrated interface of aperture *h*.

2. Construction of the crystal interface

2.1. Constituents

2.1.1. Crystal

The crystal interface is realized between two gypsum hemispheres (Fig. 1). Both hemispheres, limited here by a (120) face, are cut along the diameter plane of a crystal ball, a construction made possible by the molecular mechanics program GenMol [10].

A hemisphere is defined by two material directions, the external normal **n**=[120] to the face and a material oriented direction in the plane of the face, here **d**=[001], as shown in Fig. 2.

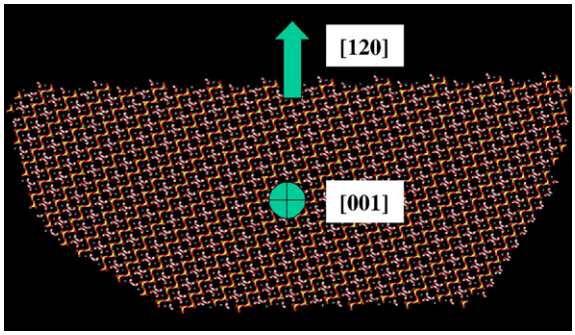

Fig. 2. Hemisphere orientation vectors **n**=[120] and **d**=[001]. (For interpretation of the references to colour in this figure legend, the reader is referred to the web version of this article.)

Table 1
Variation of atom charges in the vicinity of the (120) face

Depth	Charge Q (atom name) in e.u.								
z (Å)	Q (CA1)	Q (S2)	Q (O3)	Q (O4)	Q (O5)	Q (O6)	Q (O7)	Q (D8)	Q (D9)
$-2.8<z<=0.0$	+2.000	+1.182	−0.629	−0.629	−0.295	−0.959	−1.459	+0.245	+0.399
$-3.8<z<=-2.8$	+2.000	+1.182	−0.959	−0.295	−0.959	−0.629	−1.459	+0.245	+0.399
$-4.8<z<=-3.8$	+2.000	+1.182	−0.629	−0.629	−0.629	−0.959	−1.129	+0.245	+0.399
$-5.1<z<=-4.8$	+2.000	+1.182	−0.959	−0.959	−0.629	−0.629	−1.129	+0.245	+0.399
$z<=-5.1$	+2.000	+1.182	−0.629	−0.629	−0.629	−0.629	−1.129	+0.245	+0.399

The position of a hemisphere {**n**, **d**} is defined in an orthogonal frame (o, x, y, z) as follows:

the external normal **n** to the face is placed along axis **z**;
the oriented direction **d** is given by the oriented angle $\theta=(ox, \mathbf{d})$;
the centre of the ball is placed at $(0, 0, z_o)$.

Different interfaces of apertures $h=1$, 2, 3, 4 and 5 Å are built between the following two hemispheres:

Bottom hemisphere $\{\mathbf{n}_1, \mathbf{d}_1\}$:

$\mathbf{n}_1$ is parallel to the direction [001];
$\mathbf{d}_1$ is given by $\theta_1=(ox, \mathbf{d}_1)$;
the centre of the ball is placed at $(0, 0, z_{o1}=-h/2)$.

Top hemisphere $\{\mathbf{n}_2, \mathbf{d}_2\}$:

$\mathbf{n}_2$ is parallel to the direction [00−1];
$\mathbf{d}_2$ is given by $\theta_2=(ox, \mathbf{d}_2)=\theta_1$;
the centre of the ball is placed at $(0, 0, z_{o2}=+h/2)$.

The position of atoms are given by GenMol, according to the crystallographic definition of gypsum due to Schofield et al. [11].

2.1.2. Solution constituents

The interphase solution is supposed to be in communication with a free external reference solution. Confined or not, *a priori* these fluids include ions SO_4^{2-} and Ca^{2+} issued from the dissolution of the crystal.

The ion SO_4^{2-}, assumed to be symmetric, has a structure and charges given by GenMol:

average OS distance = 1.63 Å; angle OSO = 109.46°;
O atom charges = −0.795 e.u; S atom charge = 1.182 e.u.

The TIPS3P model is adopted for water molecules [12]:

average O_wH distance = 1.03 Å; angle HO_wH = 104.2°;
O_w atom charge = −0.834 e.u.; H atom charge = 0.417 e.u.

The initial distribution of molecules is built assuming the interphase to be completely filled with water at a normal density. Molecules of water are distributed on a cylindrical 3-D mesh of axis z, the distance between the O_w atoms being equal to 3.1 Å. This mesh is placed over a disk of ions between the crystal faces. When the distance between an O_w atom and any other atom is less than 2.0 Å, the water molecule is excluded.

2.2. Boundary conditions

A boundary condition is not necessary for the crystal, assumed to be rigid. For the fluid, the number of molecules or ions is kept constant by an impervious membrane, materialized by fixed O_w of water molecules. However, interactions between the crystal faces must be estimated taking into account a sufficient environment. In the present case, the most attractive approach seems to be a 2-D (x, y) periodic boundary, the periodicity being non existent in the z-direction. However such periodicity must preserve the periodicity of the crystal. If the periodicity of the bottom face is preserved, this is no longer the case in general for the top face (Fig. 1) and the idea of periodic boundaries has to be abandoned. Finally, the procedure adopted consists of creating a sufficiently large amount of atoms to mimic the vicinity of a central sample on which interactions are computed, as shown in Fig. 1.

2.3. Interactions and cut-off

2.3.1. Coulomb interactions

The distribution of the charges on the crystal atoms are required for Molecular Mechanics calculations between atoms belonging either to the crystal and/or the fluid. These charges are

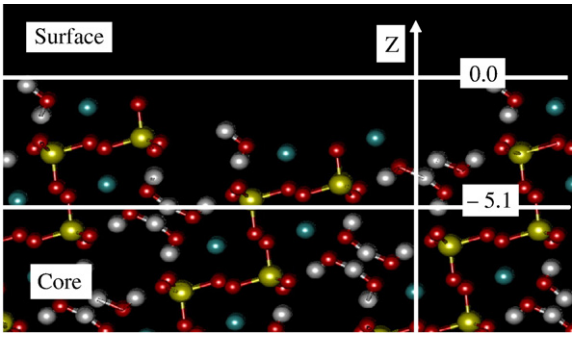

Fig. 3. Zoom on the periphase of a (120) face, Ca (cyan), S (yellow), O (red) and H (white) as shown by VMD software [see reference [20]]. (For interpretation of the references to colour in this figure legend, the reader is referred to the web version of this article.)

Table 2
Results synthesis of the inverse problem SASP++

(1)	(2)	(3)	(4)	(5)	(6)	(7)
h (Å)	Number N_w	Number N_a	Number N_b	Ratio N_b/N_a	Ratio N_a/N_w	Ratio N_b/N_w
Aperture of the interface	H_2O	Ca^{2+}	SO_4^{2-}	SO_4^{2-}/Ca^{2+}	Ca^{2+}/H_2O	SO_4^{2-}/H_2O
h=2 Å	3650	38	0	0	1.0%	0%
h=3 Å	3712	38	0	0	1.0%	0%
h=4 Å	3704	52	14	0.27	1.4%	0.4%
h=5 Å	4061	151	60	0.40	3.7%	1.5%
h infinite	/	/	/	1	0.02%	0.02%

proposed by GenMol according to Mulliken's theory [13]. The π charges and the formal charges are added to the σ charges [14]. The net charges are calculated using the Pariser–Parr method [15,16] and the formal charges are calculated by the Del Ré method [17–19]. At the periphase of an hemisphere, GenMol modifies the charges in function of the depth z (Table 1) as shown in Fig. 3. When the whole system is built, including crystal, ions, water molecules and boundaries, it is necessary to verify that the total charge is zero. However no specific modification of charges is made when placing together crystal atoms and fluid ions or molecules. Similarly, no possible covalent bonds are envisaged between the crystal and the fluid atoms.

2.3.2. Other interactions

The parameters of covalent potentials and van der Waals potentials (R^{-6}, R^{-12}) are extracted from CHARMM libraries [21] or Xplor [22]. All these parameters are supposed to be valid at the ambient conditions.

2.3.3. Cut-off and switch

Interactions between far distant atoms are generally excluded or attenuated by cut-off and switch functions. Such functions were adopted to optimize the position equilibrium of the interphase constituents by a conjugated gradient algorithm in the NAMD software [23]. After several tests, a cut-off of 12 Å was adopted with an 8 Å switch-parameter. However, after optimization of the interphase solution, computation of the interaction energy is realized between the top and the bottom sample, the limits of the model (Fig. 1) controlling perfectly the neighborhood of the sample.

3. Mass equilibrium

3.1. Recalling the methodology

The mass equilibrium of the interphase, as described in Section 3.2 below, is based on the identity between the chemical potential μ_k of any constituent k within the interphase and within the free external solution. Consequently, a prerequisite consists of finding chemical potentials within the free external solution. In the following, as in reference [9], the composition of the free saturated $CaSO_4$ solution is supposed to be known and equal to 13.4 mmol l^{-1} at ambient temperature. Hence, chemical potentials of the free solution can be extracted from reference [9] (Section IIIB "Case study A: Direct problem SASP applied to a free saturated gypsum solution", Table 2). The composition and structure of the confined solution within the interface can be obtained as described in reference [9] (Section IVC "Case study C: Inverse problem SASP++ on an interphase solution"), the classical or partial chemical potentials in the interphase being

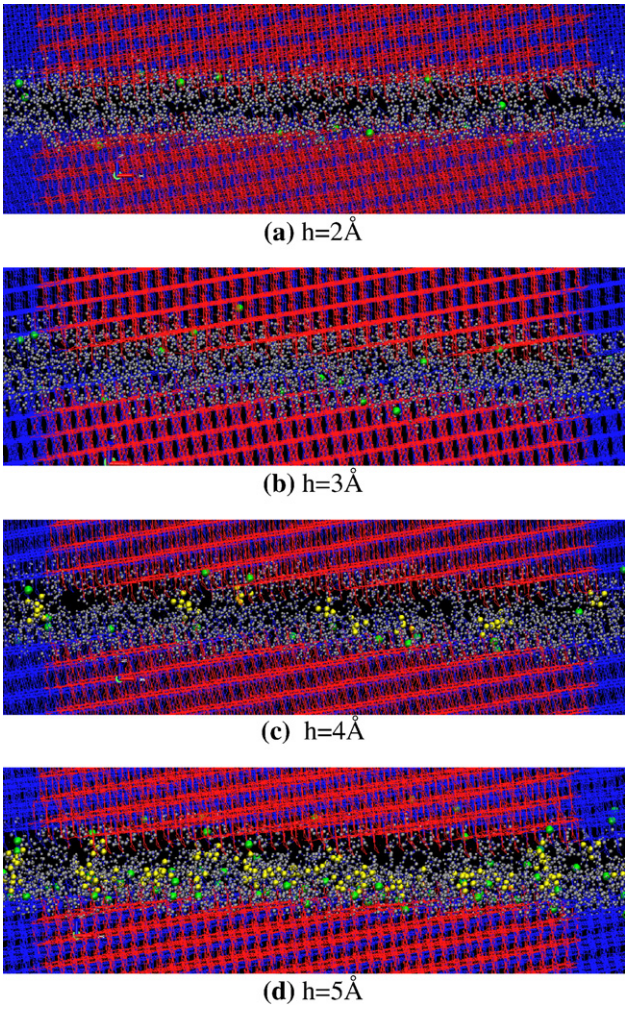

Fig. 4. Particle distribution in the interphase between (120) gypsum faces in the central part (red) of the sample at different apertures h [H_2O (silver), SO_4^{2-} (yellow), Ca^{2+} (green)]. (For interpretation of the references to colour in this figure legend, the reader is referred to the web version of this article.)

equal, at equilibrium, to the chemical potentials of the free solution. The principle of the SASP (Semi Analytical Stochastic Perturbations) method is summarized in the Appendix at the bottom of the paper.

3.2. New results

Case study C cited above was treated using a 3 Å interface. In view of the mechanical problem, this case study was extended to 2 Å, 4 Å and 5 Å interfaces using the same methodology. For $h=1$ Å where the ion mobility is reduced, the number of ions is assumed to be similar to the case $h=2$ Å. The results are provided in Table 2. An image of the positions of atoms belonging to ions and water molecules is given in Fig. 4a,b,c and d, for $h=2$ Å, 3 Å, 4 Å and 5 Å respectively. Big silver spheres are representing positions of O atoms and tiny silver spheres positions of H atoms belonging to H_2O molecules. Yellow spheres are representing positions of S atoms or O atoms belonging to SO_4^{2+} ions. Position of Ca^{2-} ions are in green. (For interpretation of the references to colour in this figure legend, the reader is referred to the web version of this article.) Covalent bonds between atoms are not represented at this scale. It could appear surprising to have so many ions or water molecules between faces separated by very small h "distances", especially under 3 Å. It has to be realized that (120) faces at the atomic scale are very "rough", with "groves" which may be as deep as 2 to 3 Å. Aperture h is conventionally defined as the distance separating two fictitious planes passing through the centre of "crest" atoms. For instance for $h=1$ Å, the free space for ions or water molecules can be of 4 to 5 Å between "groves".

3.3. New observations

The first major observation concerns the ratio (N_b/N_a) of the number N_b of SO_4^{2-} ions to the number N_a of Ca^{2+} ions. The lack of SO_4^{2-} ions within a 3 Å interface was reported in reference [9] (Section IVC, Fig. 10a). The new results show that sulfate ions are present within the interphase as soon as h is larger than 3 Å. The ratio (N_b/N_a) increases with h from 0 ($h=3$ Å) to 1 ($h\to\infty$) within a free solution. The results at 4 Å and 5 Å give a preliminary idea of the variation of this ratio for increasing h values as shown in Fig. 5. To confirm the extrapolation curve, a systematic investigation of larger h values would be necessary,

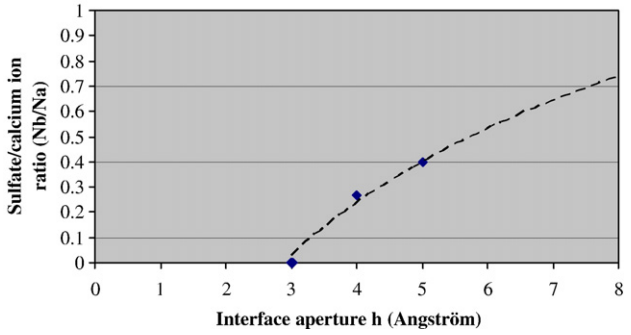

Fig. 5. Ratio of sulfate ions/calcium ions, versus interface aperture h.

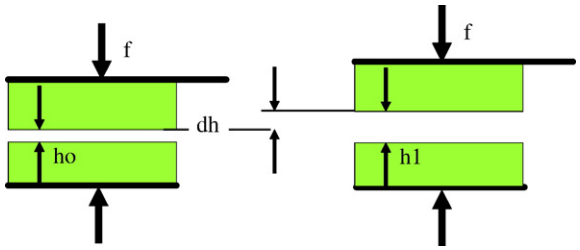

Fig. 6. Virtual displacement dh.

but this is beyond the demonstrative scope of the present paper centred around the value $h=3$ Å, where experimental A.F.M. tests [7,24] show a maximum of adhesion for a (120)/(120) gypsum interface. The second major observation is that the ratio (Ca^{2+}/H_2O) and also the ratio (SO_4^{2-}/H_2O) above 3 Å are much higher within the confined interphase than in the free solution. Thus it would be entirely wrong to assume an equal concentration of the confined and the free solutions.

4. Momentum equilibrium

4.1. Method

4.1.1. Interaction effort

Assuming the mass equilibrium of an interface of aperture h to be achieved, it is necessary to apply an external force **f** acting on the top and a reverse force −**f** applied to the bottom of the crystal sample to maintain the mechanical equilibrium, as in A.F.M. tests. These opposite forces are characterized by the effort f, a number equal to the modulus of these two forces, with a conventional sign, here (+) if the faces are repulsive and (−) if they are attractive. To evaluate this effort f, an infinitesimal virtual displacement dh (Fig. 6) is applied leading to the following variation of energy and free energy of the crystal faces, considered as a "solid system", the solution being not a part of it but considered as the outside environment:

$$dE = TdS - fdh + \sum_s \mu_k dN_k \quad (1)$$

$$dF = -SdT - fdh + \sum_s \mu_k dN_k \quad (2)$$

with:

E=energy of the crystal; F=free energy of the crystal; T=temperature;
S=entropy of the crystal; μ_k=chemical potential of species k in the crystal;
N_k=number of atoms of species k in the crystal.

This transformation does not affect the number of atoms in crystal hemispheres and thus $dN_k=0$. This virtual infinitesimal transformation is isothermal, thus $dT=0$. Moreover, as the crystal hemispheres are assumed to be rigid along this virtual transformation, the variation of entropy $dS=0$. In this special

case, the variation of energy dE is equal to the variation of free energy dF, formulae (1) and (2) being reduced to:

$$dE = TdS - fdh + \sum_k \mu_k dN_k = -fdh \quad (1bis)$$

$$dF = -SdT - fdh + \sum_k \mu_k dN_k = -fdh \quad (2bis)$$

leading to the effort f by one of the following derivatives:

$$f = -\frac{\partial E}{\partial h} = -\frac{dE}{dh} = -\frac{\partial F}{\partial h} = -\frac{dF}{dh}. \quad (3)$$

To confirm this approach of the effort f, an alternative consists of applying the mechanical theorem of virtual work to a virtual displacement dh of the crystal faces, because this transformation of the "solid system" is purely mechanical ($dN_k=0$) without any thermal or chemical evolution. This theorem states that, in the vicinity of a momentum equilibrium position of a mechanical system, the work of internal plus external forces in any virtual displacement is equal to zero. This theorem can be applied to the equilibrium of the crystal faces considered as the "solid system", in presence of the solution considered as the environment of the system, the aperture h being maintained constant by external forces **f** which counterbalance the attraction or repulsion forces $-$**f**. Thus the momentum equilibrium of the solid system is the result of internal interactions between atoms, belonging to either crystal faces, external forces coming from the solution, plus the imposed external forces **f**. During a virtual displacement dh, the variation of energy dE=dF includes the internal work relative to the solid system and the external work relative to the solution. This work variation, added to the virtual work fdh of the external stabilizing forces (opposite to the work of the attraction or repulsive forces – fdh), must be equal to zero. Thus dE+fdh=dF+fdh=0. This identity is similar to expression (3).

A second possibility is to consider a "total system" including the crystal faces plus the solution. Formulae (1) and (2) become for this "solid+solution system":

$$dE_{tot} = TdS_{tot} - fdh + \sum_s \mu_s dN_s \quad (4)$$

$$dF_{tot} = -S_{tot}\, dT - fdh + \sum_s \mu_s\, dN_s \equiv -fdh + \sum_s \mu_s\, dN_s \quad (5)$$

with:

E_{tot}=energy of the crystal+solution; F_{tot}=free energy of the crystal+solution;
T=fixed temperature; S_{tot}=entropy of the crystal+solution;
μ_s=chemical potential of species s in the crystal or solution;
N_s=number of atoms of species s in the crystal or solution;
μ_s=corresponding chemical potentials.

Here the single possible simplification comes from dT=0 in formula (5). However, keeping the above assumptions for the crystal, during a virtual displacement dh a variation of entropy dS_{tot} is due to the variation of the solution entropy only. Similarly the variations dN_s of the number of atoms is due to the evolution of the concentration of the solution only. For these two reasons, considering this global system which is no longer a pure mechanical system induces two main drawbacks:

- First of all, it is no longer possible to identify dE_{tot} with dF_{tot}, due to the term dS_{tot} which is introduced by the variation of entropy of the solution in the expression of dE_{tot}. Formula (5) appears to be simpler than (4) for obtaining f, but it requires computing the free energy variation dF_{tot}.
- Moreover, after obtaining dF_{tot}, the estimation of f derived by relation (5) imposes the computation of the chemical term $\sum_s \mu_s dN_s$.

Finally, advantages of considering the "solid system" only, instead of the "solid+solution system", are the following:

- For the "solid system", due to the identify dE=dF, it is possible to compute energy E only, without being obliged to compute free energy F. Such a simplification is not valid for the global system, dF_{tot} being different from dE_{tot}.
- Considering the "solid system" provides a clear separation between chemical equilibrium and momentum equilibrium where a pure mechanical approach is possible for estimating directly f as a total derivative of E with respect to h, without taking into consideration any complementary chemical term $\sum_s \mu_s dN_s$.

4.1.2. Interaction energy E

Interaction energy E between two faces is the sum of potentials acting on atoms belonging to the crystal samples on each side of the interphase. The potential of one atom, belonging for instance to the top sample (see Fig. 7), includes the contributions U1 from other atoms of the top hemisphere, U2 from atoms of the bottom hemisphere and U3 from atoms of the interphase solution. Thus an atom belonging to the top or bottom samples is subjected to contributions from atoms belonging to the "solid system" (U1 and U2) and atoms outside the "solid system" (U3). Covalent terms in U1 and U2 remain constant in all

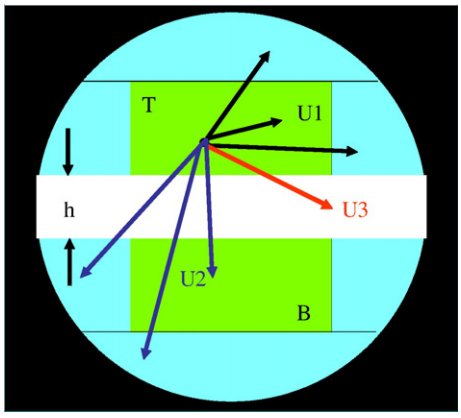

Fig. 7. Potential contributions to the energy of one atom of the top sample. (For interpretation of the references to colour in this figure legend, the reader is referred to the web version of this article.)

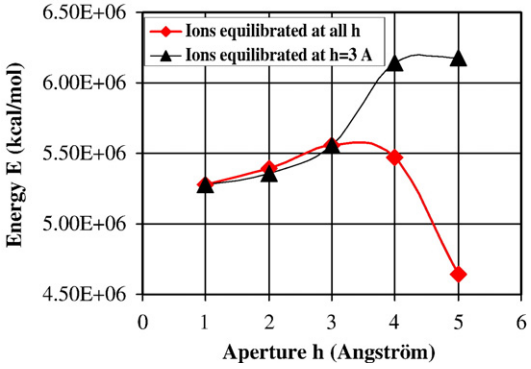

Fig. 8. Interaction energy E versus interface aperture h.

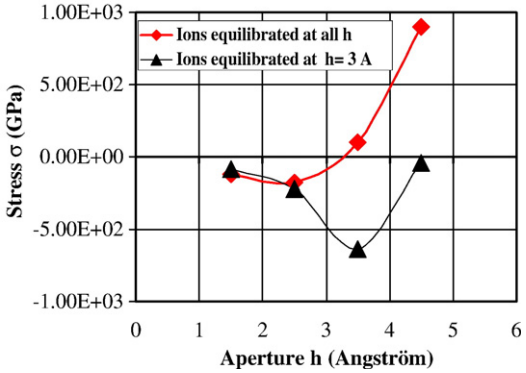

Fig. 10. Interaction stress σ versus interface aperture h.

numerical experiments, the crystal being assumed to be rigid. Covalent terms in U3 are ignored, assuming that no covalent bonds occur between ions and the crystal faces. Under these assumptions, the variations of the interaction energy include only non bond terms. A special code was developed for a precise calculation of above interactions, without any cut-off or switch functions. It has to be underlined that this code computes values of E only and not values of E_{tot} because it does not take into account internal interactions between atoms within the solution.

4.1.3. Interaction stress

The interaction stress $\sigma = f/s$ is immediately accessible by molecular simulation because the cross section "s" of the samples is well defined (see Fig. 1). The above convention of signs on f leads to the following convention: $\sigma > 0$ for repulsion and $\sigma < 0$ for attraction.

4.1.4. Adhesion

Adhesion between two faces corresponds to a state where the attraction between faces is maximum. Two parameters (h_o, σ_o) are sufficient to characterize intrinsic adhesion:

(i) The critical interphase thickness h_o;
(ii) The absolute value of the stress necessary for separating two faces, defined as the adhesion stress σ_o.

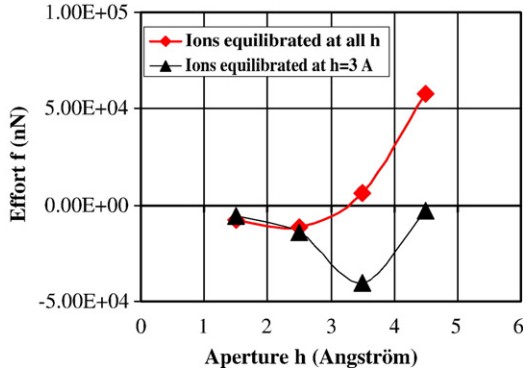

Fig. 9. Interaction effort f versus interface aperture h.

4.2. Results

The interaction energy E is given in Fig. 8, for apertures between 1 and 5 Å, taking into account the ions distribution equilibrated for each aperture h of the interface as derived in Section 3. However, in order to investigate the importance of the composition of the interphase solution, another series of result is given, in which the number of ions is kept artificially constant in all interfaces and equal to the number of ions obtained for $h = 3$ Å. The interaction effort f, shown in Fig. 9, is obtained by differentiating the energy curve. The corresponding interaction stress σ is given in Fig. 10, taking into account a cross section of the sample $s = 63.61$ nm^2.

4.3. Discussion

4.3.1. Possible comparison with experimental results

The correct results, with ions and water molecules in equilibrium for each aperture h, lead to the following adhesion characteristics:

Critical aperture $h_o \approx 2.5$ Å
Maximum attraction effort $f_o \approx -1.15E4$ nN
Maximum attraction stress $\sigma_o \approx -1.8E2$ GPa

Validating these numerical results by comparison with A.F.M. tests seems possible for the critical aperture. Experiments reported by Finot [7,24] between a gypsum tip and gypsum (120) face indicate a critical aperture in the vicinity of 3 Å. This comparison is excellent, taking into account the difficulty of defining a distance between two faces, either numerically or experimentally. In contrast, comparing efforts would require a complete simulation at scale 1 of the tip and the base of the experimental A.F.M. test; this would be far from the present simulation between ideal parallel (120) gypsum faces. The comparison between stresses appears in principle to be easier but it is experimentally very difficult to realize ideal parallel faces and then to measure the "contact area".

4.3.2. Virtual simulation

An unexpected observation is the radical difference between results where the mass equilibrium of ions is correct and the

virtual simulation assuming the ions concentration to remain stable when the aperture varies around $h=3$ Å. This shows how important is a correct study of the interface solution, as obtained by the SASP inverse problem approach. This proves that a distribution of ions and water molecules within the interface obtained by approximated methods such as a semi-continuous approach, or assumptions identifying the interphase and free phase concentrations, could lead to entirely wrong results. The ratio anions/cations appears to play here a fundamental role for interpreting the adhesion process, which is related to the absence of SO_4^{2-} ions in the present case of (120) gypsum faces. As soon as the aperture is larger than 3 Å, these ions are admitted within the interface and the attraction between faces vanishes. The other parameter, i.e. the ratio ions/water molecules, certainly plays a role. However investigating the relative importance of both parameters would necessitate further virtual experiments.

4.3.3. Physical interpretation of energy, forces and stress graphs

The $\sigma(h)$ stress-strain graph can be interpreted exactly as in a traction test under an *imposed increasing deformation*. The maximum resistance occurs when the slope of the energy curve is maximum, i.e. at the inflexion point of the energy curve $h\approx 2.5$ Å. (Values of effort f or stress σ are obtained by finite derivation of the energy curve, this fact explaining why h values are not integer values as for energy). After this peak of attraction, when the distance between faces increases, the attraction between the faces decreases down to zero ($h\approx 3.5$ Å). For an imposed larger aperture $h>3.5$ Å, a repulsion appears between the faces. Physically speaking, attraction between faces is stabilized by Ca^{2+} ions and destabilized by intrusion of SO_4^{2-} ions. In a test, under an *imposed increasing traction* $\sigma(h)$, a sudden decohesion phenomenon is observed when the resistance of the sample becomes smaller than the imposed stress. The maximum of the energy curve is the signature of an instable situation between adhesion and repulsion. In contrast, the minimum of the energy curve, in the vicinity of $h=1$ Å, corresponds to a zero stress, for an equilibrium state where the faces are in "contact". Physically, due to "roughness" of the (120) faces, Ca^{2+} ions are still present with some remaining water molecules.

4.3.4. Induced consequences at a macroscopic scale

Above atomic scale results require attention before to be transposed at the macroscopic level. Basically, a fundamental difference must be made between "adhesion" stresses (hundreds of GPa) at the atomic scale and "cohesion" stresses (some MPa) at the macroscopic scale. Indeed, high adhesion stresses in closed interfaces are not alone and coexist with high repulsion stresses between larger interfaces as shown in Fig. 9. Thus cohesion, at the macroscopic scale, is the consequence of the competition between both types of atomic interactions. Their integration in a structure at the macroscopic scale leads either to a material with cohesion or a cohesionless material. Another result which appears surprising is the small number of ions and molecules remaining at equilibrium between attracting crystal faces. This appears to be in contradiction with the large number of water molecules or ions remaining in a wet- or even air dried-cohesive gypsum sample. In fact, a significant number of ions and molecules can remain at a macroscopic scale between crystallites, whereas few ions or water molecules are subsisting at "contacts" between crystallites responsible for adhesion. Many other complex phenomena at the macroscopic scale, such as the additive action, can be enlightened by a careful interpretation of atomic modeling results.

5. Synthesis and trends

The investigation of sub-nanocrystal interfaces, of apertures less than 10 Å, including a fluid interphase in equilibrium with a free solution, is possible thanks to the SASP algorithm. This technique leads to results in sub-nanochemistry and sub-nanomechanics of solids and fluids, which could not be obtained by any meso or macro approach. The first issue is to confirm by a quantitative study that the chemical composition of sub-nano-phases, as encountered in very confined interfaces, is radically different from the composition of free phases. The parity between ions and cations is no longer assured, and the ratio of ions to water molecules is totally different from the free solution. For instance, it is not possible to speak of solubility product within confined solutions, where uniformity of macro-scale solutions disappears due to repelled or attracted ions by crystal faces. The second issue confirmed by a virtual simulation is that sub-nanomechanics between crystal faces, in presence of a solution, is governed not only by the type of crystal faces but is also strongly coupled with the chemical equilibrium of the interphase fluid, requiring a correct and very precise estimation of the ions distribution within the interphase. Finally the third issue concerns the consequences of atomistic insights, obtained by molecular modeling, for understanding engineering properties such as the macroscopic cohesion.

A purely numerical determination of the composition of a solution in equilibrium with a crystal, under any temperature T and pressure P, was still an open problem when reference [9] was published, impeding a complete numerical treatment of the inverse problem without the help of experimental data for the free solution. It should be mentioned that this limitation has now been overcome by a generalized inverse SASP process [25], not yet published in a review. The latter development, including chemical reactions and phase changes, between crystals and free or confined solutions, whatever the number of constituents, provides a general approach for applications in macro or nanochemistry and related mechanical or thermal applications.

Molecular mechanics introduces covalent interactions. However such covalent bonds cannot be created or deleted between atoms during an optimization or molecular dynamics process. In the case of gypsum, it is admitted that strong ionic forces are hindering possible covalent character modifications. Anyway if some covalence contribution would exist at the contact between crystal and fluid, it would contribute to reinforce the present adhesion forces at small distances between the faces and thus confirm the attraction between faces at small distances. Only *ab initio* computations would exhibit evolution of electronic orbitals.

Presently *ab initio* codes are specialized in either crystals (CASTEP, VASP, CRYSTAL,…), fluids (CPMD,…) or isolated molecules (GAUSSIAN,…). Efforts are done for coupling *ab initio* crystal modeling with molecular mechanics in fluids (cp2k,…). However such a QMMM approach, with more than 300 000 atoms as in the present study, is judged by the best experts too early a project.

Acknowledgments

The authors are grateful to André Nonat, who gave us access to the Laboratoire de Recherche sur la Réactivité des Solides (L.R.R.S.) and the Laboratoire de Physique de l'Université de Bourgogne (L.P.U.B.), specialists in gypsum and cement materials. For computations we are grateful to the authors of GenMol and NAMD softwares, and for visualization to the authors of the VMD software. This work was supported by the C.N.R.S. and the Fonds National de la Science, France. Finally we thank both unknown reviewers of this paper whose comments lead to a refined discussion of physical consequences induced by molecular modeling.

Appendix A. Principle of the SASP method

Direct SASP method

In a canonical situation, the direct SASP+problem consists of obtaining the chemical potentials $\mu_1(T, V, N_1, N_2,\ldots N_k,\ldots N_n),\ldots \mu_k(T, V, N_1, N_2,\ldots N_k,\ldots N_n),\ldots \mu_n(T, V, N_1, N_2,\ldots N_k,\ldots N_n)$ of the different species $k(=1, n)$ of a given free solution, when the number of particles $(N_1, N_2,\ldots N_k,\ldots N_n)$ is fixed within a volume V at temperature T. Under these conditions, at the thermodynamical limit, the chemical potential μ_k of species k is defined as the derivative of the free energy F in function of the parameter N_k, all other variables T, V and N_j ($j\neq k$) being fixed. To compute this partial derivative, two twin elementary perturbations $(0, 0,\ldots \pm \mathrm{dn}_k,\ldots 0)$, relative to each species k, are generating twin perturbed states, one state "plus" $(T, V, N_1, N_2,\ldots N_k+\mathrm{dn}_k,\ldots N_n)$ and one state "minus" $(T, V, N_1, N_2,\ldots N_k-\mathrm{dn}_k,\ldots N_n)$. After optimization of both perturbed states, the corresponding free energies noted F_{k+} for the state "plus" and F_{k-} for the state "minus" are computed by molecular modeling. A first order discrete derivative gives the chemical potential μ_k:

$$\mu_k = \frac{F_{k+} - F_{k-}}{2\mathrm{dn}_k}. \tag{A1}$$

This analytical result includes stochastic effects due to the arbitrary choice of numbers dn_k of particles to be added or withdrawn to the initial state and their arbitrary choice, which explain the acronym SASP used for Semi Analytical Stochastic Perturbation method. The expectation value of the chemical potential is given by the mean of μ_k.

In fact, instead of these conventional chemical potentials μ_k used in the SASP+method, authors have defined, in the SASP++ method, the so-called "partial chemical potentials" μ_{kk}. They are defined starting from the partial free energies $F_k(T, V, N_1, N_2,\ldots N_k,\ldots N_n)$ of species k, instead of the free energy $F(T, V, N_1, N_2,\ldots N_k,\ldots N_n)$ of the total solution including all species, by:

$$\mu_{kk} = \frac{F_{kk+} - F_{kk-}}{2\mathrm{dn}_k} \tag{A1bis}$$

The free energies F_{kk+} and F_{kk-} are the free energies computed for two twin perturbed states $(N_1, N_2,\ldots N_k\pm\mathrm{dn}_k,\ldots N_n)$ associated with the initial state $(N_1, N_2,\ldots N_k,\ldots N_n)$, obtained by modifying by $\pm\mathrm{dn}_k$ the number of particles of the species k, without modifying the volume of the considered domain. It is important to note that this concept of partial free energy is not accessible by experimental means. It is used here in view of reducing the computation time and increasing the precision of computation, in particular when the concentration of ions is very small.

Inverse SASP method

The inverse problem examined here consists of finding the average number of particles of the different species within a solution in volume V at temperature T, where chemical potentials of each species k are given at equilibrium. The inverse SASP approach treats this problem by a semi analytical and stochastic iteration process. The SASP+ version presented below can be can be readily transformed into the SASP++ version using above definition (A1bis).

The *analytical aspect* of an iteration is based on the following Taylor's development:

$$\mu_k^t(T, V, N_1^t,\ldots N_k^t,\ldots N_n^t) = \mu_k(T, V, N_1,\ldots N_k,\ldots N_n) + \sum_{j=1}^{n} \frac{\partial \mu_k}{\partial N_j}\mathrm{dN_j} + O(\mu_k^2), (\forall k = 1, n) \tag{A2}$$

with the following notations:

- The numerical vales of $\mu_k(T, V, N_1,\ldots N_k,\ldots N_n)$ at the equilibrium state So are given, but the corresponding composition $(N_1,\ldots N_k,\ldots N_n)$ is ignored and is the target of the inverse problem.
- Any iteration process starts from an initial state $S^t(T, \mathrm{V}, N_1^{\mathrm{t}}, N_2^{\mathrm{t}},\ldots N_k^t\ldots N_n^t)$. Corresponding chemical potentials $\mu_k^t(T, V, N_1^t, N_2^t,\ldots N_k^t,\ldots N_n^t)$ are computed by a direct process based on formulae (A1).
- Main derivatives $\frac{\partial \mu_k^t}{\partial N_k}$ are approximated by:

$$\frac{\partial \mu_k^t}{\partial N_k} = \frac{\mu_{k(+)}^t - \mu_{k(-)}^t}{\mathrm{dn}_k} = \frac{F_{k+}^t - 2F^t + F_{k-}^t}{\mathrm{dn}_k \mathrm{dn}_k} \tag{A3}$$

Finally the remaining unknowns are the difference in composition $(\mathrm{dN_1}, \mathrm{dN_2},\ldots \mathrm{dN_k},\ldots \mathrm{dN_n})$ between the non equilibrium state S^t and the wanted equilibrium state So, plus the cross derivatives $\varepsilon_{kj} = \frac{\partial \mu_k^t}{\partial N_j}$. A first estimation N_{k}^1 of the unknown composition at equilibrium N_k, equal to $N_k^t - \mathrm{dN_k}$, is obtained by

solving n-linear equations, where the ε_{kj} terms are considered of second order:

$$\begin{vmatrix} N_1^1 \\ N_2^1 \\ N_3^1 \\ \dots \\ N_k^1 \\ \dots \\ N_n^1 \end{vmatrix} = \begin{vmatrix} N_1^t \\ N_2^t \\ N_3^t \\ \dots \\ N_k^t \\ \dots \\ N_n^t \end{vmatrix} - \mathrm{Inv} \begin{vmatrix} \frac{\partial \mu_1^t}{\partial N_1^t} & \varepsilon_{12} & \varepsilon_{13} & \dots & \varepsilon_{1k} & \dots & \varepsilon_{1n} \\ \varepsilon_{21} & \frac{\partial \mu_2^t}{\partial N_2^t} & \varepsilon_{23} & \dots & \varepsilon_{2k} & \dots & \varepsilon_{2n} \\ \varepsilon_{31} & \varepsilon_{32} & \frac{\partial \mu_3^t}{\partial N_3^t} & \dots & \varepsilon_{3k} & \dots & \varepsilon_{3n} \\ \dots & \dots & \dots & \dots & \dots & \dots & \dots \\ \varepsilon_{k1} & \varepsilon_{k2} & \varepsilon_{k3} & \dots & \frac{\partial \mu_k^t}{\partial N_k^t} & \dots & \varepsilon_{kn} \\ \dots & \dots & \dots & \dots & \dots & \dots & \dots \\ \varepsilon_{n1} & \varepsilon_{n2} & \varepsilon_{n3} & \dots & \varepsilon_{nk} & \dots & \frac{\partial \mu_n^t}{\partial N_n^t} \end{vmatrix} x \begin{vmatrix} \mu_1^t - \mu_1^r \\ \mu_2^t - \mu_2^r \\ \mu_3^t - \mu_3^r \\ \dots \\ \mu_k^t - \mu_k^r \\ \dots \\ \mu_n^t - \mu_n^r \end{vmatrix} \tag{A4}$$

Neglecting the ε_{kj}'s, the above matrix leads to a first approximation $(N_1^1, N_2^1, \dots N_k^1, \dots N_n^1)$ of the number of particles:

$$N_k^1 = N_k^t - \frac{\mu_k^t - \mu_k}{\frac{\partial \mu_k^t}{\partial N_k^t}}, \quad (\forall k = 1, n) \tag{A5}$$

This first approximation of the particle distribution is followed by a succession of iterations, where the new initial state corresponds to the last approximated state. The process converges when above approximations are becoming negligible.

Different stochastic aspects are imbricated with the above analytical aspect. First of all, the initial state $(N_1^t, N_2^t, \dots N_k^t, \dots N_n^t)_{j=1}$ at iteration $j=1$ before starting a set of iterations is arbitrary. A second stochastic aspect consists of choosing arbitrarily the number and positions of particles involved in the $2n$ elementary perturbations $(0,0,\dots \pm \mathrm{d}n_k, \dots 0)$ used in formula (A1).

Possible generalization

The inverse SASP approach is applied here in a special case where all chemical potentials of the different species are supposed to be known at equilibrium. In such a case, even if it appears equivalent to a Grand Canonical Monte-Carlo (GCMC) method, the SASP approach has the advantage to allow a rapid convergence in presence of a very large number of particles — in particular when all the solvent molecules are represented instead of simulating the solvent by a continuous fluid-, without any limitation of concentration or interaction with boundaries. However the most interesting feature of the SASP approach is probably its generalization [25] for solving equilibria including chemical reactions with mass conservation constraints, in contrast with a classical GCMC method no longer operating when chemical potentials at equilibrium are *a priori* partially or totally ignored.

References

[1] D. Tabor, R.H.S. Winterton, Nature 219 (1968) 1120.
[2] B.V. Derjaguin, Y.I. Rabinovich, N.V. Churaev, Nature 265 (1977) 520.
[3] J.N. Israelachvili, Intermolecular and Surface Forces, 2nd ed. Academic, New York, 1991.
[4] E.D. Shchukin, E.A. Amelina, Contact interaction in disperse systems, Adv. Colloid Interface Sci. 11 (1979) 235–287.
[5] L. Meagher, J. Colloid Interface Sci. 152 (1992) 293–295.
[6] E. Finot, E. Lesniewska, J.-P. Goudonnet, J.-C. Mutin, Study of forces between microcrystals of gypsum by atomic force microscopy, 2nd International RILEM Workshop on Hydration and Setting, 1997, pp. 117–134.
[7] E. Finot, E. Lesniewska, J.-C. Mutin, J.-P. Goudonnet, Investigations of surface forces between gypsum crystals in electrolytic solutions using microcantilevers, J. Chem. Phys. 111 (14) (1999) 6590–6598.
[8] P. Jouanna, L. Pedesseau, G. Pepe, Towards prediction of the impact of admixtures on the interaction between hydrated crystals by molecular modelling. Case study of (120)/(120) gypsum faces in solution with citric acid, Euromat 2003, Topic: P Building Materials; P1 Nanoscience of Cementitious Materials, 1–5 September 2003, Lausanne: Paper 1716, 2003.
[9] L. Pèdesseau, P. Jouanna, Phases, periphases, and interphases equilibrium by molecular modeling. I. Mass equilibrium by the semianalytical stochastic perturbations method and application to a solution between (120) gypsum faces, J. Chem. Phys. 121 (24) (2004) 12511–12522.
[10] G. Pèpe, GenMol, Version January 1998, GCOM2, Faculté des Sciences de Luminy, Université de la Méditerranée, case 901, 163 Avenue de Luminy, 13288 Marseille Cedex 9, France, 1998.
[11] P.F. Schofield, K.S. Knight, I.C. Stretton, Thermal expansion of gypsum investigated by neutron powder diffraction, Am. Mineral. 81 (1996) 847–851.
[12] W.L. Jorgensen, J. Chandrasekhar, J.D. Madura, R.W. Impey, M.L. Klein, Comparison of simple potentials functions for simulating liquid water, J. Chem. Phys. 79 (2) (1983) 926–935.
[13] R.S. Mulliken, Electronic population analysis on LCAO-MO molecular wave functions, J. Chem. Phys. 23 (10) (1955) 1833–1846.
[14] J. Langlet, P. Claverie, F. Caron, J.-C. Boeuve, Interactions between nucleic acid bases in hydrogen bonded and stacked configurations: the role of the molecular charge distribution, Int. J. Quant. Chem. 20 (2) (1981) 299–338.
[15] R. Pariser, R.G. Parr, A semi-empirical theory of the electronic spectra and electronic structure of complex unsaturated molecules. II, J. Chem. Phys. 21 (5) (1953) 767–776.
[16] G. Pèpe, B. Serres, D. Laporte, G. Del Ré, C. Minichino, Surface electrostatic potentials on macromolecules in a monopole approximation: a computer program and an application to cytochromes, J. Theor. Biol. 115 (1985) 571–593.
[17] G. Del Ré, A simple MO-LCAO method for the calculation of charge distributions in saturated organic molecules, J. Chem. Soc. 40 (1958) 4031–4040.
[18] G. Del Ré, B. Pullman, T. Yohezawa, Electronic structure of the amino acids of proteins: I. Charge distributions and proton chemical shifts, Biochem. Biophys. Acta 75 (1963) 153–182.
[19] G. Del Ré, G. Berthier, J. Serre, Electrons States of Molecules and Atoms Clusters, Springer Verlag, Heidelberg, 1980.
[20] W. Humphery, A. Dalke, K. Schulten, VMD version 1.4b4 — Visual Molecular Dynamics, J. Mol. Graph. 14.1 (1996) 33–38.
[21] B.R. Brooks, R.E. Bruccoleri, B.D. Olafson, D.J. States, S. Swaminathan, M. Karplus, CHARMM: a program for macromolecular energy, minimization and dynamics calculations, J. Comp. Chem. 4 (1983) 187–217.
[22] A.T. Brünger, X-PLOR (Version 3.1), A System for X-ray Crystallography and NMR, Yale University Press, New Haven, Connecticut, 1992.
[23] L.V. Kale, R. Skeel, M. Bhandarkar, R. Brunner, A. Gursoy, N. Krawetz, J. Phillips, A. Shinozaki, K. Varadarajan, K. Schulten, NAMD2: greater scalability for parallel molecular dynamics, J. Comput. Phys. 151 (1999) 283–312.
[24] E. Finot, Mesure des forces intercristallines à l'origine de la prise du plâtre par microscopie à force atomique, Thèse de Doctorat, Laboratoire de Physique de l'Université de Bourgogne, 23 janvier 1998, Dijon, France, Fig. 8.3B, p. 146. (1998).
[25] P. Jouanna, Approche phéno-corpusculaire de phases et nanophases. Voies ouvertes en sciences des géomatériaux, Thèse de Doctorat, 14 décembre 2005, Université Montpellier II, Montpellier, France.